VILNIUS UNIVERSITY
SEMICONDUCTOR PHYSICS INSTITUTE OF CENTRE FOR PHYSICAL SCIENCES AND TECHNOLOGY

MARIUS TREIDERIS

FORMATION AND INVESTIGATION OF HYBRYD NANOSTRUCTURES

Summary of doctoral dissertation
Technological sciences, materials engineering (08T)

VILNIUS, 2011

Doctoral dissertation was prepared at Semiconductor Physics Institute of Centre for Physical Sciences and Technology in 2006-2011.

Scientific Supervisor:
Assoc. Prof. Habil. Dr. Irena Šimkienė (Semiconductor Physics Institute of Centre for Physical Sciences and Technology, Technological Sciences, Materials engineering - 08T)

Scientific Consultant:
Prof. Habil. Dr. Gintautas Jurgis Babonas (Semiconductor Physics Institute of Centre for Physical Sciences and Technology, Physical Sciences, Physics - 02P)

The dissertation will be defended at the Council of Technological sciences of Vilnius University:

Chairman

Prof. Dr. Gintaras Valusis (Semiconductor Physics Institute of Centre for Physical Sciences and Technology, Physical Sciences, Physics - 02P)

Members:

Prof. Dr. Habil Antanas Feliksas Orliukas (Vilnius University, Technological Sciences, Materials engineering - 08T),

Prof. Dr. Habil Rimantas Ramanauskas (Institute of Chemistry of Center for Physical Sciences and Technology, Physical Sciences, Chemistry – 03P),

Prof. Dr. Diana Adlienė (Kaunas University of Technology, Technological Sciences, Materials engineering - 08T),

Assoc. Prof. Dr. Arūnas Setkus (Semiconductor Physics Institute of Centre for Physical Sciences and Technology, Technological Sciences, Materials engineering - 08T).

Oponents:

Prof. Dr. Habil Donatas Rimantas Vaišnoras (Vilnius Pedagogical University, Physical Sciences, Physics - 02P),

Assoc. Prof. Dr. Bonifacas Vengalis (Semiconductor Physics Institute of Centre for Physical Sciences and Technology, Technological Sciences, Materials engineering - 08T).

The dissertation will be defended at the public meeting of the Council of Technological sciences in the Hall of Semiconductor Physics Institute of Centre for Physical Sciences and Technology at 2 p.m. on 27th of September in 2011. Address: A. Gostauto 11, Lt-01108 Vilnius, Lithuania.

The summary of doctoral dissertation was distributed on 26th of August in 2011. A copy of the doctoral dissertation is available for review at the Library of Semiconductor Physics Institute of Centre for Physical Sciences and Technology and at the Library of Vilnius University.

VILNIAUS UNIVERSITETAS
FIZINIŲ IR TECHNOLOGIJOS MOKSLŲ CENTRO PUSLAIDININKIŲ FIZIKOS INSTITUTAS

MARIUS TREIDERIS

HIBRIDINIŲ NANODARINIŲ FORMAVIMAS IR TYRIMAS

Daktaro disertacijos santrauka
Technologiniai mokslai,medžiagų inžinerija (08T)

VILNIUS, 2011

Disertacija rengta 2006 - 2011 metais FTMC Puslaidininkių fizikos institute

Mokslinis vadovas:

Doc. habil. dr. Irena Šimkienė (Fizinių ir technologijos mokslų centro Puslaidininkių fizikos institutas, technologijos mokslai, medžiagų inžinerija - 08T)

Konsultantas:

Prof. habil. dr. Gintautas Jurgis Babonas (Fizinių ir technologijos mokslų centro Puslaidininkių fizikos institutas, fiziniai mokslai, fizika - 02P)

Disertacija ginama Vilniaus Universiteto Technologinių mokslų srities medžiagų inžinerijos krypties taryboje:

Pirmininkas

Prof. dr. Gintaras Valušis (Fizinių ir technologijos mokslų centro Puslaidininkių fizikos institutas, fiziniai mokslai, fizika – 02P).

Nariai:

Prof. habil. dr. Antanas Feliksas Orliukas (Vilniaus universitetas, technologiniai mokslai, medžiagų inžinerija – 08T),

Prof. habil. dr. Rimantas Ramanauskas (Fizinių ir technologijos mokslų centro Chemijos institutas, fiziniai mokslai, chemija – 03P),

Prof. dr. Diana Adlienė (Kauno technologijos universitetas, technologiniai mokslai, medžiagų inžinerija – 08T),

Doc. dr. Arūnas Šetkus (Fizinių ir technologijos mokslų centro Puslaidininkių fizikos institutas, technologiniai mokslai, medžiagų inžinerija – 08T).

Oponentai:

Prof. habil. dr. Donatas Rimantas Vaišnoras (Vilniaus pedagoginis universitetas, fiziniai mokslai, fizika – 02P),

Doc. dr. Bonifacas Vengalis (Fizinių ir technologijos mokslų centro Puslaidininkių fizikos institutas, technologiniai mokslai, medžiagų inžinerija – 08T).

Disertacija bus ginama viešajame Technologijos mokslų srities medžiagų inžinerijos krypties tarybos posėdyje 2011m. rugsėjo mėn. 27 d. 14 val. Fizinių ir technologijos mokslų centro Puslaidininkių fizikos instituto posėdžių salėje. Adresas: A. Goštauto g. 11, LT-01108 Vilnius, Lietuva.

Disertacijos santrauka išsiuntinėta 2011 m. rugpjūčio 26 d.

Disertaciją galima peržiūrėti Fizinių ir technologijos mokslų centro Puslaidininkių fizikos instituto ir Vilniaus universiteto bibliotekose.

Introduction

Moore's law describes the evolution of the semiconductor industry in the 20 and 21 centuries. According to this law or some other representations of this law, the changes in technology and future steps are predicted. However, there is an important task to decide what technology or what the processes are worth (in economic terms) the funds allocated for their research. To solve this problem, the International Technology Roadmap for Semiconductors [1] was created. It is supported by Europe, Japan, Korea, Taiwan and the U.S. Semiconductor Industry Associations. The basic idea of this roadmap is that in the future of the semiconductor industry, technologies, which reduce the size of the smallest cells for the materials that are already used, will be important. Also, it is important to search for new materials to build a new type of devices that could be used for the systems SiP (System in Package) and SoC (System on Chip). These innovations lead to the nanotechnology and new hybrid structures. Reducing of manufacturing cost is important, too.

Over the past decade, the intensive development of nanotechnology was made to increase significantly the number of methods to form the structures of a size between 1 and 100 nm. It should be emphasized that nanostructured materials are interesting both because of perspectives in practical applications and new physical phenomena.

The cheap chemical methods that do not require special equipment for synthesis of nanostructures are most promising [2]. One of the methods for chemical synthesis of semiconductor nanostructures is electrochemical etching. This is a low-cost technology that can compete with the methods that use expensive technological equipment for the formation of nanostructures. Another advantage of the chemical technology is that high density nanocrystalline coatings and micro or nanopore layers on the semiconductor substrates can be formed for the passivation of optoelectronic devices. The pores can be filled with metals, semiconductors and bio-molecules to form the hybrid structures suitable for photonics, sensors, bio-sensors, optical filters, catalysts, bioreactors and other new generation devices [3,4].

Another method of chemical synthesis is used for the formation of porous silicate dielectric layers by sol-gel technology [5]. Silica gel and aerogel are known since the third decade of the last century, but in recent years these materials became very relevant. Research on porous aerogels has shown large application possibilities. For instance, nano-sized pores regularly ordered in silicon oxide glass can be used as photonic structures and in the integral circuits as excellent thermal insulators with low dielectric constant. Filling the nanopores with metals or semiconductors enables one to form the hybrid nanostructures, which are new multiphase materials with new physical properties. Such hybrid structures with nano-sized inclusions formed by low-cost low-temperature technology are currently very important and hold a prominent place in nanotechnology today. Most of the technological research is carried out with macro-sized materials. Therefore, the formation of thin-film dielectric nanoporous layers on a wide variety of substrates, including the silicon substrate dominating in planar technology, is very important. Taking into account the relevance of the technologies mentioned above, the aims and objectives of the present work was formulated.

Aim of the work

The aim of this work is to develop the well-controlled chemical and electrochemical methods for the formation of materials with nanometer-sized elements on porous dielectric or semiconductor basis, to characterize such materials by their physical properties and to propose their practical use.

Tasks of the work

To develop the electrochemical technique for the control of morphology of porous silicon matrix.

To form the hybrid transition metal/por-Si structures and to study their morphology and optical response.

To develop the method for infiltration of biomolecules into the porous silicon structures and to study the interaction between silicon and bio-molecules.

To study the formation of GaP nanostructures by electrochemical etching and to investigate the possibilities of their application for gas sensors.

To investigate the formation of nanoporous and Fe-doped silica and to characterize the developed structures by their structural, optical or magnetic properties.

Scientific novelty

The formation technology of morphology-controlled porous silicon layers was designed by using the 1.2 μm light illuminating the etched surface or the bottom side of the substrate. The technology for the formation of organic-inorganic hybrid nanostructures on the basis of porous Si was developed. The main regularities in the interaction between Si surface and porphyrin were revealed.

The dependence of the morphology of electrochemically formed porous GaP on technological parameters was determined. The GaP nanorods were formed for the first time by using electrochemical etching in nitric acid with organic solvent.

Iron/ iron oxide nanoparticles and clusters in SiO_2 thin-layer matrix were formed and the iron charge state was found to depend critically on the essential features of precursor and the annealing atmosphere.

Thesis statements

1. The morphology of porous n-Si layer depends essentially on the illumination during the electrochemical etching. This dependence is determined by light-generated holes. At illumination of the etched surface, the holes are generated between the pores, thus enhancing the branching of the pores. When the backside of substrate is illuminated, the holes are generated uniformly, hence the pores grow in depth uniformly with the diameter unchanged.

2. The formation of por-Si-based hybrid structures is determined by the insertion of biomolecules with sulfate functional groups into the pores and the linkage by covalent bonds with silanol groups on the pore surfaces.

3. By using the electrolyte of nitric acid with an organic solvent, the GaP nanorods (~100 nm in diameter and 3-10 μm in height) can be formed by electrochemical etching. Nanorods originate from por-GaP, when the walls of pores thin, their resistance

increases and the etching rate decreases. The whole etching process of por-GaP consists of the following sequence of morphological changes: pores in GaP matrix - honeycomb - nanorods.

4. The properties of Fe/Fe-O nanoparticles formed in porous SiO_2 matrix by sol-gel technique, depend essentially on the annealing atmosphere. In spite of oxide environment in thin matrix layer containing free oxygen, annealing in oxidising and inert atmospheres at 550^{o}C favors the formation of Fe oxide nanoparticles whereas metal Fe nanoclusters develop in a reducing atmosphere.

Structure of the dissertation

The dissertation (in Lithuanian) includes introduction, 4 chapters, general conclusions, list of publications and references.

The introduction describes the relevance of dissertation, the aim and tasks of the work, scientific novelty and thesis statements.

1. Methods for sample characterization

The morphology of composite structures was investigated by scanning electron microscopes (SEMs) BS 300, SUPRA 35 and EVO 50 EP (Carl Zeiss SMT) and atomic force microscope (AFM) Thermomicroscope Explorer and Dimension 3100/ Nanoscope IVa (Veeco Metrology Group).

For characterization of the optical properties of hybrid structures, Nicolet 8700 FT-IR spectrometer was used for FTIR measurements, Horiba Jobin Yvon spectrometer for Raman scattering studies, SOPRA GES 5 for spectral ellipsometry and LEF-3M for null-ellipsometry.

Magnetic properties of hybrid structures were studied using a commercial SQUID magnetometer MPMS-5 (Quantum Design).

2. Hybrid nanostructures ir porous Si matrix

In this chapter the formation of porous silicon structures and hybrid structures is discussed. Also, experimental results on the characterization of the structures are summarized.

n-por-Si samples were fabricated using (100)-oriented wafers of n-Si (0.5 Ω·cm) as substrates. Before etching, the wafers were degreased by dimethyl formamide, washed by methanol and deionized water and dried with hot air. Porous layers were produced by electrochemical etching in electrolyte HF:C_2H_5OH (1:1) at 3-35 mA/cm^2 for 1-60 min. The upper layer, which is responsible for photoluminescence of por-Si and is composed of Si nanocrystals imbedded in oxide matrix, was removed with 30% KOH aqueous solution.

Samples were etched illuminating different parts of the substrates. The backside surface or the etched interface were illuminated with 100 W incandescent lamp (λ = 1.2 μm).

Thin silicon membranes were made using (100)-oriented wafers of p-Si (1 Ω·cm). The wafers of thickness 480 and 380 μm were used. Before etching the wafers were degreased by dimethyl formamide, washed by methanol and deionized water and dried with hot air. Prior to electrochemical etching, the substrates were chemically etched with

CP-4A (HNO_3: HF: CH_3COOH = 3:1:1) or CP-8 (HNO_3: HF = 3:1). Etching was carried out for 30 to 40 minutes. Electrochemical etching was processed in the same cell as that for fabrication of n-por-Si, but instead of aluminum foil the graphite plate was used for better electrical contact. Porous layers were produced by electrochemical etching in electrolyte HF:C_2H_5OH (1:1) at 3-35 mA/cm^2 for 1-60 min. The upper layer was removed with 30% KOH aqueous solution.

The por-Si structure was infiltrated with Ni and Co by electrochemical technique. Por-Si with infiltrated Ni was formed using electrolyte of composition $NiSO_4O$ (250 g/L): Na_2SO_4 (100 g/L): H_3BO_3 (10 g/L): 1 M $C_4H_6O_6$. In this electrolyte, anions are stable therefore Ni-ion complexes are not formed. The electrolyte acidity (pH 4) was controlled by boric acid. Organic component, tartaric acid, improved the metal adhesion on Si surface. During electrochemical process, the current density was equal to 1.5 mA/ cm^2 at deposition time which was varied in the range from 2 to 60 s. For Co deposition the electrolyte $CoSO_4 \cdot 7H_2O$ (75 g/L): $CaH_{15}NO_3$ (70 mL/L) with pH 2.6 was used at

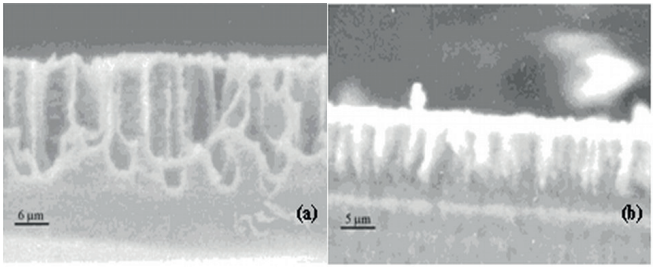

Fig. 1. SEM micrographs of por-n-Si (upper luminescent layer removed), (a) before and (b) after infiltration of Ni.

current density 10 mA/cm^2 and deposition time 360 s.

The por-Si structures were also infiltrated with porphyrins using the aqueous solution of porphyrin of concentration 1 x 10^{-4} M, which has been prepared by dissolving meso-tetra(4-sulfonatophenyl)porphine ($TPPS_4$) tetrasodium salt. Adding 0.1 M HCl, the solution of pH=1 was made. In the aqueous medium of this acidity the J-aggregates are formed. The samples were stored at room temperature for 10 days to achieve a stable state with respect to the formation of large J-aggregates. The drop of this solution was deposited on por-Si.

The morphology of por-n-Si depends strongly on the technological procedure. At higher current densities, the pores, which have been formed in the substrate, are randomly distributed with their size varying from 1 to 5 μm. At lower current densities with backside illumination (Fig. 1(a)), the pores are cylindrically-shaped. According to AFM data, the distance between pores varies in the range of 1-5 μm and the surface roughness is of the order of 0.5 μm. The cross-sectional image illustrates the thickness of porous layer which is equal to 18 pm for a particular sample shown in Fig. 1(a). After electrochemical deposition of transition metal (Fig. 1(b)), the surface of por- n-Si was coated by a metal layer and pores were partially filled with metal nanostructures. In order to reveal the particular features of the pores in substrate, the sample of por-n-Si was polished to remove the upper metal layer.

The optical properties of initial and fabricated por- n-Si samples were investigated by measuring optical response using null-ellipsometry technique at 633 nm. Measured and calculated ellipsometric angular dependence of ellipsometric parameters is presented in Fig. 2. These results were analyzed using the three-layer c-Si/por-Si (Ni, Co)/air model. For comparison, the Si substrate and the porous Si layer without top layer measurement results are presented in Fig. 3.

Analysis of ellipsometric results using three-layer model showed that the n-Si

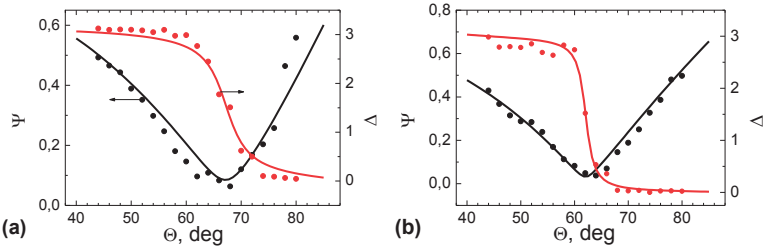

*Fig. 2. Experimental and modeled angular dependence of ellipsometric parameters for hybrid samples of (a) por-**n**-Si:Ni and (b) por-**n**-Si:Co.*

substrates were coated with 5-6 nm thick SiO_2 layer. The porosity of etched porous layer on the substrate was 0.5 to 0.7. From the effective media model analysis of ellipsometric data for hybrid samples it followed that Ni and Co concentration in the samples was 5-10%.

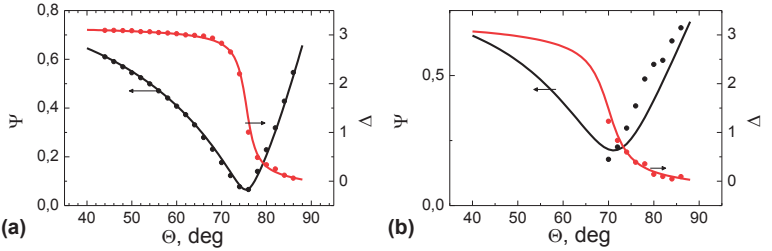

Fig. 3. Angular dependence of ellipsometric parameters for (a) initial sample of c-Si and (b) for por-n-Si with removed surface layer.

For por-Si structures with infiltrated Ni the effective layer thickness of 300 nm was estimated and the chemical composition 0,36:0,55:0,09 Si, air and Ni, respectively, was determined. As for the porous layer with infiltrated Co, the effective thickness of 1 μm, and the composition 0.22, 0.07 and 0.71 for Si, Co and air, respectively, were obtained. As it is seen, the effective thickness of the layer calculated from ellipsometric data is less than the porous layer thickness. This value depends on the structural model. In the present case, the model with cylindrical pores was accepted.

The analysis of null-ellipsometry data has confirmed the structural results

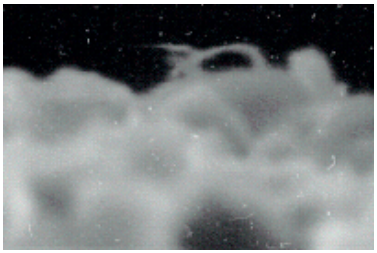

Fig. 4. SEM image of por-Si formed in HF:C_2H_5OH=1:1, j=3 mA/cm^2, t=15 min., illuminated from top, infiltrated with $TPPS_4$.

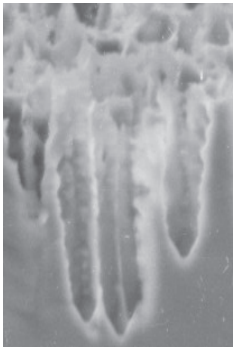

Fig. 5. SEM image of por-Si formed in HF:C_2H_5OH=1:1, j=15 mA/cm^2, t=15 min., illuminated from top, infiltrated with $TPPS_4$.

indicating the occurrence of transition metal formations in the pores of hybrid por-n-Si (Ni, Co) structures, the concentration of which can be determined ellipsometrically with the accuracy of 3-5%.

The structure of hybrid samples composed of por-Si infiltrated with porphyrins is illustrated in Figs. 4 to 8. The technological process was based on the assumption that $TPPS_4$ aqueous solution would make a link to the hydrophilic por-Si surface and the J-aggregates would remain in the pores. As it is seen from SEM images (Fig. 4, 5), the $TPPS_4$ wires were formed in por-Si with one end of the wire fixed at the bottom of the pore.

Also, the hybrid structures composed of $TPPS_4$-infiltrated thin silicon membranes were fabricated (Fig. 6). P-type silicon substrates were chemically etched to thickness 50 to 100 μm, then the pores of 10-20 nm in size were electrochemically formed and infiltrated with aqueous solution of porphyrin aggregates. The infiltration was made by putting a drop of porphyrin solution on the membrane in ultrasonic bath. SEM images of this sample are shown in Figs. 7 and 8. As it is seen, at the drop

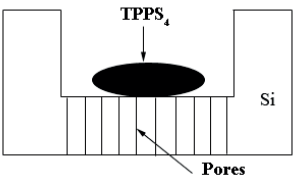

Fig. 6. Thin silicon membrane.

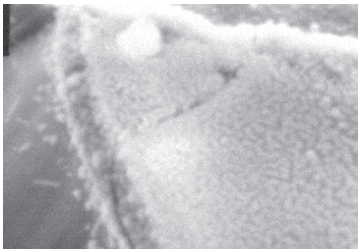

Fig. 7. SEM image of por-Si formed in HF:C_2H_5OH=1:1, 5 min. 120 mA/cm^2; 47 min. 40 mA/cm^2, without illumination, infiltrated with $TPPS_4$.

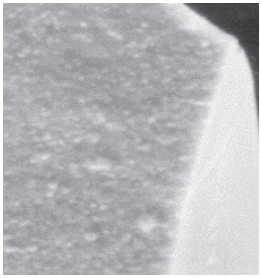

Fig. 8. SEM image of por-Si formed in HF:C_2H_5OH=1:1, 5 min. 120 mA/cm^2; 47 min. 40 mA/cm^2, without illumination, infiltrated with $TPPS_4$.

center the porphyrin aggregates of ~1 μm in width and a few micrometers in length were formed. At drop edges, the aggregates of a lower concentration were noticed (Fig. 7): larger pores were infiltrated with porphyrin (empty pores in SEM patterns are dark spots). An insertion of porphyrin aggregates into por-Si was confirmed by optical measurements.

The results of optical studies are illustrated by Figs. 9 and 10. Fig. 9 curve 2 illustrates the optical response of the sample that was made with the deposition of 0.1 mL $TPPS_4$ 1.0 × 10-4 M concentration of water solution on the por-Si. The upper oxide

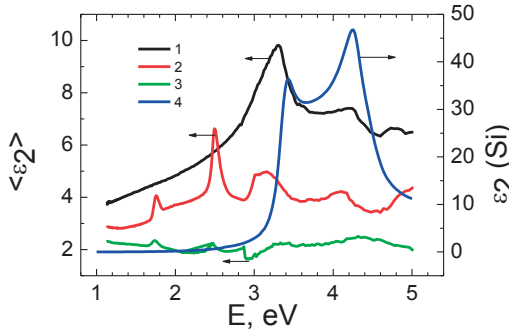

Fig. 9. Optical spectra of por-Si with removed oxide layer(1), hybrid samples of $TPPS_4$ on por-Si with removed oxide layer (2), same hybrid samples after surface polishing (3) and c-Si substrate (4).

layer was removed by etching in KOH solution. This spectrum was compared with the optical response of the surface without porphyrin (fig. 9 curve 1). As can be seen, the difference is very strong, because the response of surface with porphyrin is determined by characteristic porphyrin bands at ~ 1.8 and 2.5 eV. When the surface of complex

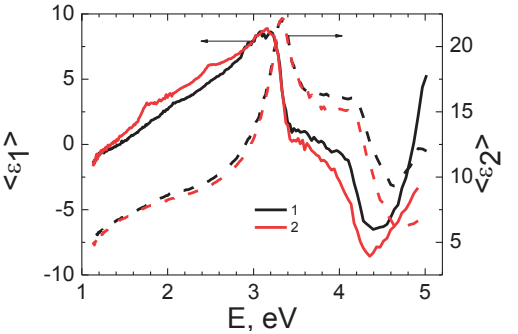

Fig. 10. Pseudodielectric function spectra of as-grown por-Si (1) and hybrid sample of $TPPS_4$ deposited on por-Si (2).

formation of Si and porphyrin was slightly (on the material) polished, the porphyrin absorption bands remained (fig. 9 curve 3). This suggests that $TPPS_4$ not only located on the por-Si substrate, but remains in pores too.

Optical response of sample produced from por-Si placing a same as before amount of $TPPS_4$ on porous layer is shown in Figure 10. As can be seen, in this case, the difference of optical response of hybrid sample and por-Si isn't very big as in previous cases, although the characteristic absorption bands of porphyrin is quite well seen. It should be noted that the differences between the spectra also occurs in the higher photon energy 3.5 - 5 eV.

Presented results indicate that por-Si layers with or without upper oxide layer were infiltrated by porphyrins and optical methods can be effectively applied to indicate porphyrins on silicon surfaces or in the por-Si pores.

3. Formation of GaP nanostructures and investigation of their properties

In this chapter the formation of porous gallium phophide is discussed. Also, the experimental results of characterization of these structures are summarized.

Por-GaP samples were prepared by electrochemical anodic etching of 300-µm-thick wafer of n-GaP with S-donor density $(5.0\text{-}5.3)\times10^{17}$ cm^{-3}. The wafers were cleaned in hot isopropyl/ethanol and washed in distilled water. Etching was carried out in dark by exposing the (111) face of c-GaP to electrolyte. The aqueous solution of 0.5M H_2SO_4, ethanol solution of 3M HNO_3 and HF:C_2H_5OH (1:1) electrolyte were used. The backside contact was made by means of In-Ga eutectics and graphite electrode. The Pt-electrode was used as cathode in the electrolyte etching cell. The etching area of GaP was 6 mm in diameter. The galvanostatic etching conditions were realized by using potentiostat Autolab PGSTAT 302 at constant current density j in the range 1-80 mA/cm^2. The etching time was 1 h.

Porous layers were formed using three different electrolytes in two different modes. At first, we will comment the structure of the samples etched at j = 1 mA/cm^2. Figure

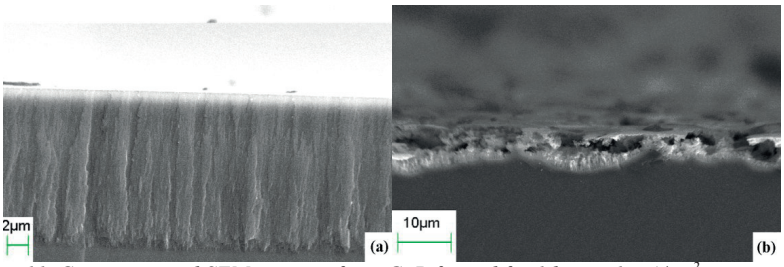

Fig. 11. Cross-sectional SEM images of por-GaP formed for 1 h at j=1 mA/cm^2 in aqueous 0.5M H_2SO_4 solution (a) and in HF: C_2H_5OH = 1:1 (b).

11a shows SEM photograph of the sample formed by using a 0.5M H_2SO_4 aqueous solution, etching time t = 1 h and 1 mA/cm^2 current density. Etching was performed in dark. The porous layer of thickness ~12-15 µm was formed. The pore size was 10-50 nm. Figure 11b represents the SEM photograph of the sample formed in the electrolyte HF: C_2H_5OH = 1:1, the etching time t = 1 h at the current density 1 mA/cm^2. The experiment was also performed in dark. The resulting thickness of porous layer was ~ 3-4 µm. The domains of pores with irregular skeleton structure were formed with domain diameter of 10 µm. Domains of leaf shape originate on the defect sites.

When 3M HNO_3 ethyl alcohol solution was used, the etching in dark for 1 h at current density 1 mA/cm^2 resulted in the formation of only the 0.5 to 1.5 μm-thick oxide layer and the porous layer did not form.

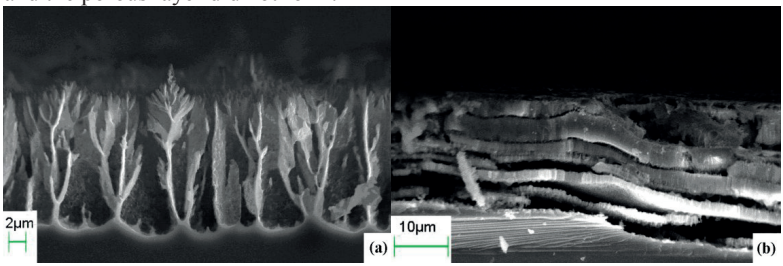

Fig. 12. Cross-sectional SEM images of por-GaP formed in aqueous 0.5M H_2SO_4 solution (a) HF: C_2H_5OH = 1:1 (b).

The structural investigations have shown that the pore size and morphology of por-GaP structures depend essentially on the type of electrolyte.

In order to determine the dependence of por-GaP morphology on the etching current, another series of samples were made at current density j = 80 mA/cm^2. Figure 12a shows the SEM photograph of the sample etched with 0.5 M H_2SO_4 aqueous solution. From SEM images (Figs. 11a and 12a), the difference in morphology of the samples etched at various current densities are clearly seen. At higher current density, the frame-type structure of pores of diameter 1-2 μm and wall thickness of ~250 nm are formed. At etching in sulfuric acid electrolyte, the pore size is limited because the frame-type structure forms. Therefore, electrolytes of other acids in organic solutions were also used. The structures of different morphology are fabricated in organic solutions. These structures have certain advantages, *e.g.*, in acid electrolytes with ethanol a surface stress is reduced because of a better watering conditions and a reduced adhesion of H_2-bubbles on the surface.

Figure 12b presents the SEM photograph of the sample etched in HF: C_2H_5OH = 1:1 electrolyte at high current value (j = 80 mA/cm^2). As it is seen, a layered structure is formed with each layer of thickness 3-4 mm and pore diameter of ~300 nm. The occurrence of separated porous layers indicates that the etching was made in a polishing mode.

For sample etched in 3M HNO_3 ethanol solution, a thick 10-20 μm porous oxide layer is formed. However, in the areas, where the oxide layer is detached from the surface, the nanorods were found. The oxide layer was removed in 30% KOH solution and nanorods of 3-10 μm in height and 100-400 nm in width became clearly visible (Fig. 13). For the first time, the GaP nanorods were formed by electrochemical etching.

In previous works it was noted that etching in 3M HNO_3 aqueous, only the oxide layer grew and porous layer did not form. However, using the 3M HNO_3 ethanol solution, the nanorods previously discussed were formed. It can be assumed that in this case the ethanol acts as a stabilizer, preventing the formation of branches and favoring an increase of pore diameter. When the pore walls become thin enough, the resistance increases significantly, and the etching rate decreases. The nanorods originate from these thin walls during the etching process. The height, diameter and concentration of nanorods depend on the etching conditions. By using different applied potentials, the nanorods of various height, width and concentration can be formed.

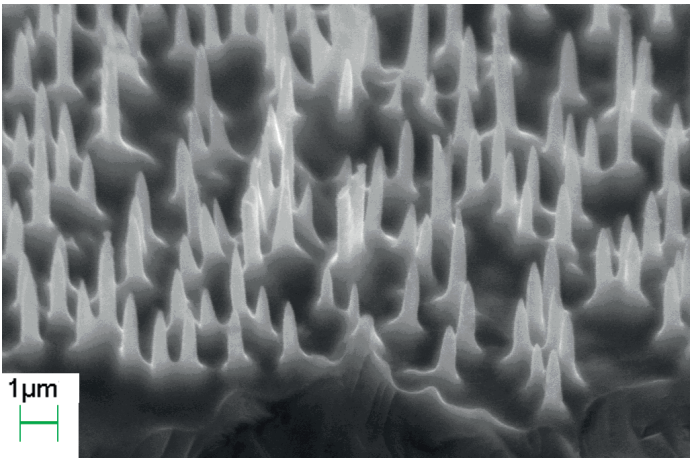

Fig. 13. GaP nanorods formed in 3M HNO_3 ethanol solution for 1 h at j=80 mA/cm^2

Typical IR reflection spectra of the investigated samples por-GaP/GaP in reststrahlen region are presented in Fig. 14. In the spectra of normalized reflection coefficient $R_{norm}(\omega)$ two bands, low- (LE) and high-energy (HE), appeared for all the samples formed in various electrolytes at small current density (1 mA/cm^2). However, the

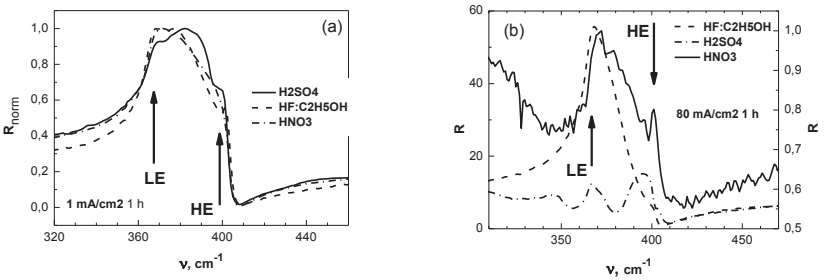

Fig. 14. Reflectance of por-GaP/GaP structures formed in various electrolytes at small (a) and large (b) current densities.

difference in lineshape is clearly seen for samples formed at j=80 mA/cm^2.

The origin of the fine structure in the reflection spectra follows from model [6] calculations (Fig. 15). The dielectric function has been calculated in the model developed for cylindrical pores in GaP with electronic dielectric function ε_∞=9.036 and the energies of TO- and LO-modes equal to 366 and 402.3 cm^{-1}, respectively. The relative volume concentration of GaP in por-GaP c and damping γ were treated as free parameters.

Thus, the LE band in dielectric function spectra ε(ω) (Fig. 15a) originates from GaP TO phonon whereas the HE band is related to GaP LO phonon (at high-energy point

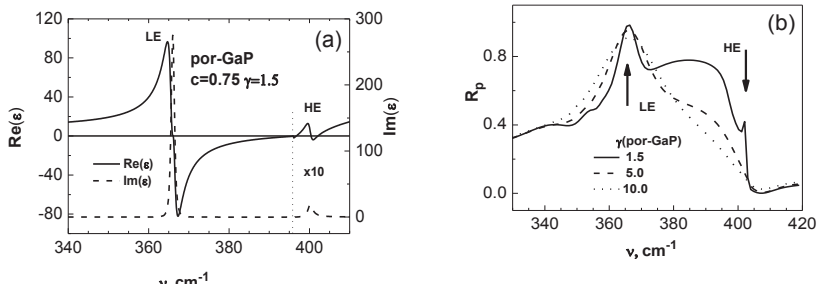

Fig. 15. Modeled dielectric function ε(ω) of por-GaP (a) and p-polarized reflectance of por-GaP(d=10μm,γ,c=0.9)/GaP(γ=0,c=1) structure at incidence angle 22^o (b).

Re(ε)=0) and to Frölich TO- and LO-modes. Depending on the combination of free parameters (c, γ) both bulk phonon and Frölich modes were seen in the modeled spectra.

Basing on the model calculations, the correlation between the reflection spectra and morphology of the samples under consideration were revealed. It should be emphasized that an increase of the damping parameter γ (Fig. 15b) as well as decrease of the volume concentration of GaP (c-parameter) results in the decrease of the HE-side of the reststrahlen band. A comparison of Fig. 14a and Fig. 14b has shown that an increase of current density in the procedure of porous layer formation leads to a change of the shape of reststrahlen band in the samples formed in HF-based electrolyte. This observation is assumed to be caused by an increase of the number of porous layers at high current densities resulting in an increase of light losses. On the contrary, the shape does not change in the samples fabricated by HNO_3 electrolyte though the intensity of reflected radiation is significantly lower in samples produced at high current density. In H_2SO_4-electrolyte samples, in the range of small current densities, the current increase leads to the increase of porous layer thickness as it is evidenced from interference pattern, but the shape of reststrahlen band is not significantly changed. However, a slight increase of illumination from dark to room illumination does not change the thickness of porous layers formed in H_2SO_4 electrolyte but the HE band is increased due to increase of free carrier concentration resulting in a higher porosity.

One of the possible practical applications of por-GaP is an organic vapor sensors. For this purpose ITO / por-GaP n-n^+ heterostructure was formed. Por-GaP was coated with a ~ 70 nm thick ITO (indium tin oxide) layer using magnetron sputtering. Ohmic contact on the backside was made coating GaP with Sn / Au by magnetron sputtering, too.

For this heterostructure the change in resistance when exposed to ethyl alcohol vapor at 9% concentration in the air was measured. Measured sensitivity was R_{air} / $R_{ethanol}$ = 1.1. These results will be used to improve the development of new sensor based on por-GaP.

Results disscused in this chapter show that the structure of por-GaP layers depends on the used electrolyte. Measured IR spectra of those layers corelate with the morfology. GaP nanorods using electrochemical etching method were formed for the first time. Also the gas sensor on por-GaP basis was demonstrated.

4. Formation and investigation of porous SiO_2 hybrid nanostructures

In this chapter formation of porous SiO_2 thin layers and hybrid structures with Fe containing nanoparticles (NPs) is discussed. Also, experimental results on characterization of these structures are summarized.

The multilayered hybrid structures (SiO_2:Fe)/SiO_2/Si were fabricated by sol-gel spin-on technique using the procedure described elsewhere [7]. For deposition of SiO_2 layers, tetraethoxysilane (TEOS) colloidal solution (pH 1.96) of composition $Si(C_2H_5O)_4$ (20 ml) : C_2H_5OH (40 ml) : H_2O (4 ml) : HCl (0.1 ml) has been prepared. A uniform silica sol was formed in 24 h at room temperature. The TEOS sol was spin-casted on cleaned Si wafer at 2500 rpm for 30 s and dried in air at 100°C for 1 h. The second SiO_2 layer was subsequently formed. The layered structure was annealed in air at 300°C for 1 h. As a result of this procedure, the SiO_2 layer of thickness 200-300 nm and porosity of 5-6 % was fabricated.

For deposition of the Fe-containing silica layer, the saturated at 20°C water solution of $FeCl_3$ was prepared. The mixture of $FeCl_3$ solution and TEOS colloidal solution at the ratio 1:1 (pH 2.5) or 1:3 (pH 5) was spin-casted for 60 s on silica-coated Si substrate and dried in air at 100°C for 30 min. The second Fe-containing silica layer was subsequently deposited and dried. In a second series of samples, one Fe-containing SiO_2 layer was formed on a bare Si substrate without the pure silica layer.

At the final stage of technological procedure, multilayered structures were annealed at 550°C for 2 h in various atmospheres: air, Ar or H_2.

Thus, the studies carried out on a series of hybrid (SiO_2:Fe)/SiO_2/Si samples prepared by the same technology allowed us to reveal a specific influence of the post-grown thermal treatment at various atmospheres.

Particular features in surface morphology are clearly seen in AFM images. The microstructure of the sample surfaces was visualized in a tapping mode. Figure 16

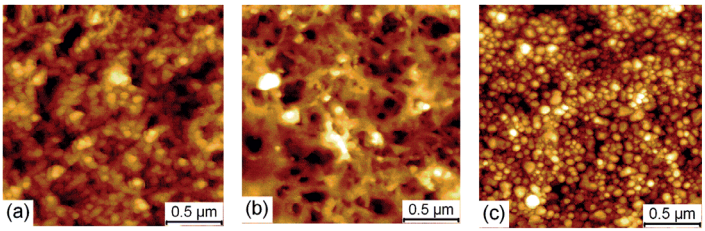

Fig. 16. AFM micrographs of (SiO_2:Fe)/SiO_2/Si structures annealed in (a) air, (b) Ar, and (c) H_2 atmosphere.

illustrates the surface structure for (SiO_2:Fe)/SiO_2/Si samples fabricated by identical technology and annealed in various atmospheres. As it is seen, the grains of the size in the range from 30 to 50 nm are formed in the samples thermally treated in air (Fig. 16a). It should be noted that simulation of AFM measurements has shown that the width of the NPs depends on the probe shape but the height does not. Therefore, a more reliable estimation of the NPs size follows from the height profile measurements. From the profile trace it is reasonable to assume that the grains observed in AFM images are composed by NPs of size 10-15 nm. The frame-like structure with wall thickness 40-80

nm is typical for the surface of samples annealed in Ar (Fig. 16b). The grains of size 30-50 nm are observed on the surface of samples annealed in H_2 atmosphere (Fig. 16c).

A small content of Fe and Fe oxides in the investigated structures (SiO_2:Fe)/SiO_2/Si makes difficult to determine directly the chemical composition of formed NPs. Nevertheless, the X-ray diffraction (XRD) data have shown the presence of hematite (α-Fe_2O_3) as the dominant phase of Fe-oxides in the samples annealed in air. In the samples annealed in Ar, the maghemite (γ-Fe_2O_3) and hematite phases were indicated though magnetite (Fe_3O_4) lines have been also noticed. In the samples annealed in H_2, metallic iron was indicated together with Fe-containing silicates like greenalite $Fe_3Si_2O_5(OH)_4$ and silicides Fe_5Si_3 and Fe_2Si.

The structural data on chemical composition of iron oxides in variously thermally treated (SiO_2:Fe)/SiO_2/Si samples were confirmed by investigations of physical properties. Below, the results of optical and magnetic measurements are presented and discussed.

For several decades, Raman and Fourier transform infrared spectroscopies have been used to characterize iron oxides [8]. Based on characteristic band frequencies and relative intensities various iron oxides and hydroxides can be easily differentiated. In addition to assignment of the oxide phases, these techniques allow one to estimate the degree of crystallinity by analysis of the parameters of the phonon modes.

In the recorded spectra, the intense band at 520.7 cm^{-1} along with a lower-intensity broad peak near 941 cm^{-1} belong to Si substrate (1st and 2nd order peaks, respectively). To obtain pure spectra of sol-gel prepared silica-Fe compounds, the difference Raman spectra were constructed by subtracting the Si contribution.

Figure 17 shows the difference Raman spectra of studied compounds. Raman spectrum observed for sample annealed in air exhibits a set of clear and strong bands typical for hematite (α–Fe_2O_3) [9] (Fig. 17a). Strong and well-defined peaks in the frequency region between 200 and 300 cm^{-1} indicate an ordered layered structure. Intense band in the vicinity of 660 cm^{-1} indicates disordering of the α–Fe_2O_3 lattice structure, which might be associated with incorporation of Si into the lattice. The broad peak near 714 cm^{-1} can not be attributed to α–Fe_2O_3. Based on previous Raman analysis of oxygenated Fe species [10], we associate this band to maghemite (γ–Fe_2O_3).

Drastic changes take place in the spectra of the sample annealed in Ar atmosphere instead of air (Fig. 17b). Bands due to α–Fe_2O_3 structure are no longer visible; instead, the intense and broad peak near 707 cm^{-1} due to γ–Fe_2O_3 compound dominates the spectrum.

By using Raman spectroscopy, we were not able to identify clearly any oxygenated Fe compounds for sample annealed in H_2 atmosphere (Fig. 17c). However, broad peaks near 1349 and 1589 cm^{-1} show the presence of nanostructured carbon at interface. These bands are resonantly enhanced, so the actual amount of carbon species might be relatively low.

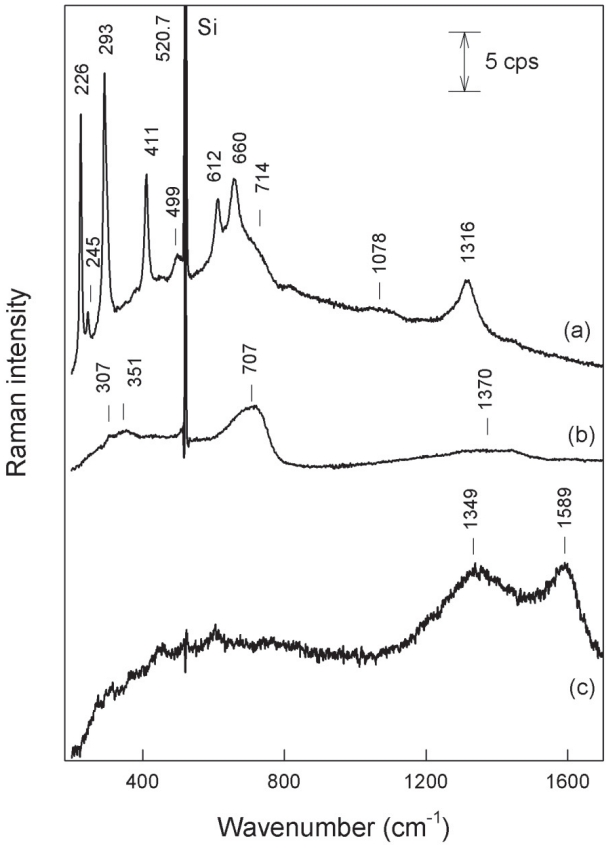

Fig. 17. Difference Raman spectra of (SiO_2:Fe)/SiO_2/Si structures annealed in (a) air, (b) Ar, and (c) H_2 atmosphere. Excitation wavelength is 632.8 nm (1 mW).

The experimental FTIR spectrum of (SiO_2:Fe)/SiO_2/Si sample annealed in air is presented in Fig. 18. The transmittance of Fe-containing sample was normalized with respect to reference sample in order to minimize the influence of silica contribution to IR spectra. In a perfect agreement with Raman data, the fine structure of transmittance spectra is well interpreted by the phonon modes typical of hematite α–Fe_2O_3 [8]. The major part of the dips in transmittance spectrum corresponds to the frequencies of IR-active TO phonon modes for hematite. For instance, the absorbance peaks at 225, 275 and 440 cm^{-1} are in agreement with corresponding peaks at 227, 286 and 437 cm^{-1} assigned to E_u-symmetry mode [8]. The peaks at 300 and 526 cm^{-1} coincide well with two TO phonon modes of A_{2u} symmetry [8]. The latter peak overlaps with TO mode of E_u symmetry which manifests itself the absorption band at 524 cm^{-1} [8].

It should be noted that, on the one hand, the surface modes are responsible for the

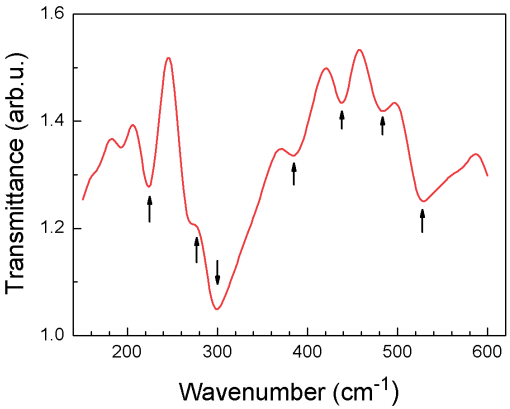

Fig. 18. Transmittance FT-IR spectrum of sample annealed in air (resolution 4 cm^{-1}) smoothed over 10 experimental points and normalized with respect to the spectrum of reference sample.

features observed for α–Fe_2O_3 thin films at frequencies between TO and LO modes [11]. In addition, a greater contribution from the LO component has been attributed to an increase in the crystallinity of hematite sample. Basing on these considerations, the absorbance peak at 385 cm^{-1} in hematite was assigned to A_{2u} phonon mode.

On the other hand, it is well established that IR spectra are dependent on the size and shape of the nanoparticles as well as on the nature of the matrix, in which the NPs are embedded. For instance, the increase of α–Fe_2O_3 nanoparticles size ranging from 18 to 120 nm shifted the E_u band with two components near 440 and 475 cm^{-1} towards higher wavenumbers [11]. From this point of view, the mode at 485 cm^{-1}, which corresponds to the peak observed in this work, was well interpreted, when homogeneous aggregation of spherical nanoparticles was taken into account.

Thus, the IR transmittance spectra of (SiO_2:Fe)/SiO_2/Si samples annealed in air correspond to those typical for hematite α–Fe_2O_3. However, the other samples were not reliably interpreted because of a smaller amount of Fe-compounds.

Spectroscopic ellipsometry presents the other non-destructive optical technique using which the composition and structure of composite multilayer samples can be efficiently investigated. The layer thickness and dielectric function of materials can be determined by analysis of the optical response of a complex structure [12]. In particular, the variable angle spectroscopic ellipsometry is useful for analysis of complex structures.

Figure 19 illustrates the experimental ellipsometric data and calculation results for the (SiO_2:Fe)/SiO_2/Si sample annealed in air. The spectra of ellipsometric parameters were simulated by a transfer-matrix technique [12]. The inverse problem was solved for three effective layers on Si substrate. The contribution of two upper layers was calculated in the effective media approximation with two constituent compounds, SiO_2 and Fe_2O_3. A surface layer of thickness ~11 nm due to surface roughness and thickness non-uniformity of ~60% have to be introduced to obtain a reasonable agreement of

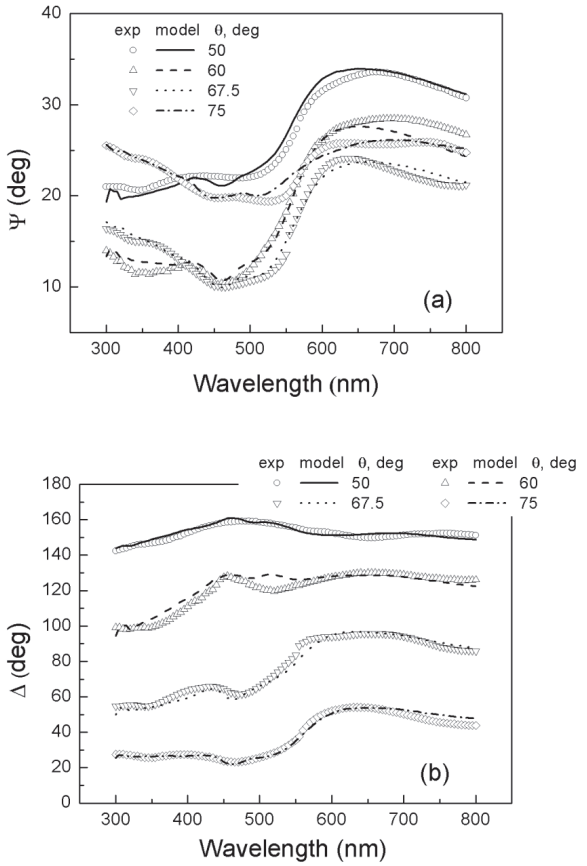

Fig. 19. Experimental (points) and calculated (curves) spectra of ellipsometric parameters Ψ (a) and Δ (b) for sample annealed in air at various angles of light incidence θ.

simulated spectra with experimental ones (Fig. 19). The analysis of ellipsometric data has shown that Fe_2O_3 is responsible for the major part of contribution to the optical response of the samples annealed in air.

Magnetic properties measurements confirm and expand optical measurements results. The magnetic field dependence of magnetization at different temperatures is shown in Fig. 20. Calculated magnetization values (~ 300 K) for samples annealed in air, argon and hydrogen is 1 × 10-5 2 × 10-5 and 2.5 x 10-4 emu respectively. Optical measurements results showed that in the samples annealed in air and argon, iron oxide particles dominate. Optical measurements couldn't tell anything about Fe-containing particles in the $(SiO_2$:Fe) / SiO_2/Si structures annealed in hydrogen. However, the

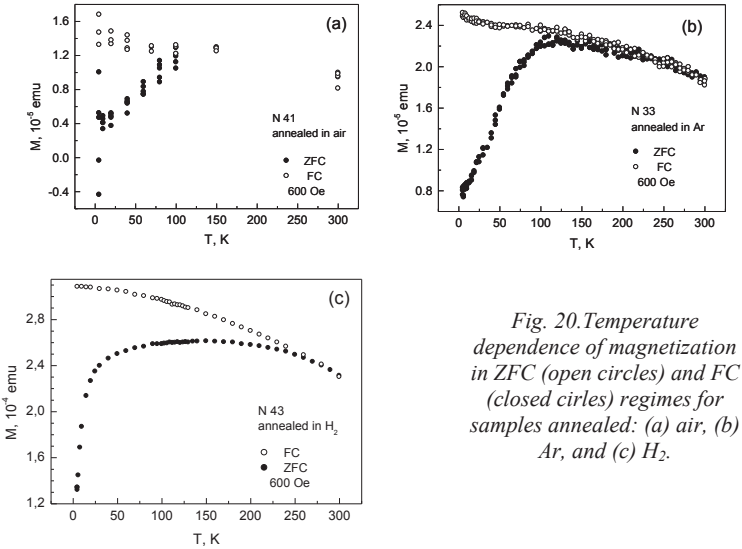

Fig. 20.Temperature dependence of magnetization in ZFC (open circles) and FC (closed cirles) regimes for samples annealed: (a) air, (b) Ar, and (c) H_2.

measured magnetization value of these samples shows that those structures consist elemental iron particles.

Result discussed in this chapter showed that chemical composition of formed NPs depends on formation technology ant annealing atmosphere. In samples annealed in air the hematite NPs was formed, annealed in argon – maghemite and in samples annealed in hydrogen the Fe NPs were formed.

General conclusions

1. Si n-type porous layer morphology depends not only on technological parameters, but also on the illumination. Illuminating the surface of the incandensend lamp (λ max = 1.2 μm, 600 lux), pores oriented perpendicular to the surface are formed. Increasing light intensity (1200 lux), the pores are branched, intertwined, and they form an irregular structure. Illuminating the sample from the substrate backside, the pores are uniform in depth, they are equal to 2.5 to 3 μm in size. Such structural differences are because of holes generated at various illumination conditions. When the etched surface is illuminated, the holes are generated in the walls between the pores and the pores became branched. While illuminating the backside of the substrates, the holes are generated uniformly at the bottom of sample and are moved towards the surface by the electric field. Then, the holes reach the bottom of pores, oxidize Si atoms. In this case, the pores grow continuously with the diameter practically unchanged.

2. Deposited from aqueous solution, the self-organization of porphyrins is different on various substrates. On a hydrophilic surface, a continuous layer of smooth J-aggregates or FeTPPS dimers is formed. On the partially hydrophobic c-Si substrates with negatively charged surface, the adsorbed positively charged aggregates with the oriented structure are

formed. Iron porphyrins on a partially hydrophobic surface formed the rings of monomers and nanoparticles of dimers inside the ring.

3. Pore size and morphology of por-GaP, formed by electrochemical etching technique, depend essentially on the type of electrolyte. When sulphuric acid and hydrofluoric acid were used at low current density, the structures typical for these electrolytes were observed. Structures etched in sulphuric acid, hydrofluoric acid and nitric acid with high current densities have been obtained for the first time. The fine structure in reflection spectra of por-GaP correlate with particular features in the morphology of the samples. For the first time, GaP nanorods were formed by electrochemical etching. A prototype of gas sensor on the basis of por-GaP/ITO was tested.

4. The sol-gel technology for the formation of controlled-porosity silicon oxide layers on crystalline silicon substrates was designed. The chemical procedure for insertion of iron and its compounds into porous SiO_2 layers was investigated. The method for iron and iron oxide formation in dielectric matrix by varying the annealing conditions was developed. It was found that forming the hybrid structures, on the one hand, the dielectric medium porosity can be controlled by changing the precursor composition and technological regimes. On the other hand, the formation of Fe/Fe-O nanostructures and clusters can be controlled by both precursor composition and annealing procedure.

Literature

1. International Technology Roadmap for Semiconductors 2005 Edition, www.itrs.net
2. V.P.Parkhutik, L.Canham, Porous silicon as an educational vehicle for introducing nanotechnology and interdisciplinary materials science, Phys. Stat. Sol. (a) **182**, 591-598 (2000).
3. R.D. Deegan, O. Bakajin, T.F. Dupont, G. Huber, S.R. Nagel, T.A. Witten, Capillary flow as the cause of ring stains from dried liquid drops, Nature **389**, 827-829 (1997).
4. P. Granitzer, K. Rumpf, and H. Krenn, Ferromagnetic nanostructures incorporated in quasi-one-dimensional porous silicon channels suitable for magnetic sensor applications, J. Nanomater. 2006, 18125 (2006).
5. C. Caiser, M. Popovici, C. Savii, Spherical $(Zn_xNi_{1-x}Fe_2O_4)_y$ nanoparticles in an amorphous $(SiO_2)_{1-y}$ matrix, prepared with the sol-gel method, Acta Materialia **51**, 3607-3616 (2003).
6. A. Sarua, J. Monecke, G. Irmer, I. Tiginyanu, G. Gartner, H. Hartnagel – Frohlich modes in porous III-V semiconductors. J. Physics: Condensed Matter **13**, 6687-6706 (2001).
7. I. Simkiene, J. Sabataityte, J.G. Babonas, A. Reza, R. Szymczak, H. Szymczak, M. Baran, M. Kozlowski, S. Gierlotka, Sol-gel processed iron-containing silica films on Si Optical Materials and Applications, ed. A.Rosental, Proc SPIE, 5946 (2005) 5946OH1-5946OH-9.
8. A.M. Jubb and H.C. Allen, Vibrational spectroscopic characterization of hematite, maghemite, and magnetite thin films produced by vapor deposition, ACS Appl. Mater. Interf. **2**, 2804-2812 (2010).

9. Ph. Colomban, S. Cherifi, and G. Despert. Raman identification of corrosion products on automotive galvanized steel sheets, J. Raman Spectrosc. **39**, 881-886 (2008).
10. S. Saremi-Yarahmadi, K.G. U. Wijayantha, A.A. Tahir, and B. Vaidhyanathan. Nanostructured α–Fe_2O_3 electrodes for solar driven water splitting: effect of doping agents on preparation and performance, J. Phys. Chem. C **113**, 4768-4778 (2009).
11. I.V. Chernyshova, M.F. Hochella, and A.S. Madden, Size-dependent structural transformations of hematite particles, Phys. Chem. Chem. Phys. **9**, 1736-1750 (2007).
12. G.J. Babonas, Elipsometrija, kn.: *Paviršiaus optinė spektroskopija*, red. V. Vaičikauskas (TEV, Vilnius, 2008) pp. 43-77.

List of Published Works on the Topic of the Dissertation

1. G.-J. Babonas, V. Snitka, R. Rodaitė, I. Šimkienė, A. Rėza, M. Treideris, Spectroscopic ellipsometry of porphyrin adsorbed in porous silicon, Acta Phys. Pol. A **107**(2), 319-323 (2005).
2. I. Šimkienė, J. Sabataitytė, A. Kindurys, M. Treideris, Formation of porous n-A_3B_5 compounds, Acta Phys. Pol. A **113**(3), 1085–1090 (2008).
3. M. Treideris, I. Šimkienė, A. Rėza, and J. Babonas, Ellipsometric studies of porous n-Si:(Co, Ni) structures, Lithuanian J. Phys. **49**(4), 439-444 (2009).
4. M. Treideris, I. Šimkienė, I. Kašalynas, A. Selskis, G. J.Babonas, Infrared reflectance of porous GaP, *Radiation interaction with material and its use in technologies. International conference (Kaunas, 2010). Program and Materials.* ISSN 1822-508X, 118-121 (2010).
5. M.Treideris, I.Simkiene, A.Selskis, Z.Balevicius and G.J.Babonas, Electrochemical formation and microstructure of porous gallium phosphide*,* Acta Phys. Pol. A **119**(2), 131–133 (2011).
6. I. Šimkienė, M. Treideris, G. Niaura, R. Szymczak, P. Aleshkevych, A. Rėza, I. Kašalynas, V. Bukauskas, G.J. Babonas, Multifunctional iron and iron oxide nanoparticles in silica, *Mater. Chem. Phys (accepted)*.

About the author

Marius Treideris was born in Vilnius on the 12th of March 1982. He took a degree of bachelor of physics in Faculty of Physics, Vilnius University, in 2004. In 2006 he received the master degree in material science in Faculty of Physics, Vilnius University. In 2006-2011 he was PhD student at Semiconductor Physics Institute. At present he is a junior research assistant in Sensors Laboratory of the Semiconductor Physics Institute of the Centre for Physical Sciences and Technology.

HIBRIDINIŲ NANODARINIŲ FORMAVIMAS IR TYRIMAS

Tiriamoji problema ir darbo aktualumas.

Pastarąjį dešimtmetį, intensyviai vystantis nanotechnologijoms, ženkliai išaugo technologinių metodų, įgalinančių suformuoti darinius, kuriuose elementų dydžiai būtų tarp 1 ir 100 nm, paieška. Šiai specifinei nanostruktūrinių medžiagų grupei skiriamas ypatingas dėmesys dėl naujų fizikinių reiškinių ir ypač - praktinių taikymų, kuriuos atveria šie dariniai.

Ypač išpopuliarėjo pigios, nereikalaujančios sudėtingos įrangos cheminės nanodarinių sintezės. Vienas iš cheminės sintezės metodų yra puslaidininkių ir jų junginių nanodarinių formavimas cheminių reakcijų praskiestuose elektrolituose metu. Tai pigi puslaidininkių ir hibridinių darinių jų pagrindu gavimo technologija, galinti konkuruoti su nanodarinių formavimu medžiagų kondensacijos būdais, kuriuose panaudojami brangūs technologiniai įrengimai. Dar vienas šios technologijos privalumas yra tas, kad priklausomai nuo technologinių parametrų galima suformuoti tankias nanokristalines dangas, pasyvuojančias optoelektroninių prietaisų paviršių, arba monokristaliniame padėkle suformuoti mikro- ar nanoporėtąjį sluoksnį, poras užpildyti metalais, puslaidininkiais ar biomolekulėmis ir paruošti hibridinius darinius, tinkamus fotonikai, jutikliams, biojutikliams, optiniams filtrams, katalizatoriams, bioreaktoriams ir kitiems naujos kartos prietaisams.

Kitas cheminės sintezės metodas – porėtųjų silikatinių dielektrinių sluoksnių formavimas „sol-gel“ technologija. Silikageliai ir aerogeliai žinomi jau nuo praeito šimtmečio trečiojo dešimtmečio, tačiau pastaraisiais metais šios nanoporėtosios medžiagos pasidarė itin aktualios. Sukurtų porėtųjų aerogelių tyrimai parodė jų žymiai platesnio taikymo galimybes: reguliariai išsidėsčiusios nanometrinio dydžio poros silicio oksidiniuose stikluose gali būti panaudotos fotonikoje, integrinėse schemose (kaip puikūs terminiai izoliatoriai su maža dielektrine konstanta), o nanoporų užpildymas pereinamais metalais ar puslaidininkiais suformuoja hibridinius nanodarinius, t.y. naujas daugiafazes medžiagas su naujomis fizinėmis savybėmis. Tokių hibridinių darinių su nanometrinio dydžio intarpais pigi, žematemperatūrinė technologija šiuo metu itin aktuali ir nanotechnologijoje užima reikšmingą vietą. Didžioji dalis technologinių tyrimų yra atliekama su tūrinėmis porėtosiomis medžiagomis. Todėl plonasluoksnių nanoporėtųjų dielektrikų formavimo ant įvairių, tame tarpe ir ant populiariausio planarinėje technologijoje silicio padėklų įsisavinimas, yra labai aktualus. Turint omenyje šių technologijų aktualumą ir buvo formuluojamas šio darbo tikslas ir uždaviniai.

Darbo tikslas. įsisavinti ir išvystyti porėtųjų dielektrikų ir puslaidininkių bei jų pagrindu hibridinių darinių su nanometrinių dydžių elementais cheminės ir elektrocheminės sintezės technologijas, kontroliuojant technologinius procesus ir charakterizuoti suformuotus darinius pagal jų sandarą ir fizikines savybes bei numatyti jų taikymo galimybes.

Darbo uždaviniai.

- elektrocheminės technologijos, skirtos kontroliuojamos morfologijos porėtojo Si matricų formavimui, sukūrimas,

- hibridinių darinių metalas/por-Si formavimas ir savybių tyrimas,
- biomolekulių įterpimo į porėtuosius silicio darinius technologijos sukūrimas bei kietakūnių padėklų sąveikos su biomolekulėmis tyrimai,
- GaP nanodarinių formavimo elektrocheminio ėsdinimo būdu dėsningumų tyrimai ir jų taikymo galimybės dujų sensoriuose,
- nanoporėtųjų dielektrinių terpių ir hibridinių nanodarinių formavimo technologijos įsisavinimas bei savybių tyrimai,
- charakterizuoti suformuotus darinius, siekiant išryškinti jų būdingas struktūrines, optines ir magnetines savybes.

Mokslinis naujumas. Sukurta kontroliuojamos morfologijos porėtojo silicio (por-Si) sluoksnių formavimo technologija, panaudojant 1,2 μm bangos ilgio apšvietimą ėsdinimo metu, apšviečiant bandinio ėsdinamą paviršių arba apatinę padėklo pusę. Sukurta organinių-neorganinių hibridinių nanodarinių por-Si pagrindu formavimo technologija.

Nustatyti porėtojo GaP (por-GaP) formavimosi dėsningumai priklausomai nuo technologinių parametrų. Azoto rūgšties organiniame tirpiklyje elektrochemiškai pirmą kartą suformuoti GaP nanostulpeliai.

Suformuotos geležies oksidų ir geležies nanodalelės plonasluoksnėje SiO_2 matricoje ir nustatyta, kad geležies būsena nanodalelėse ir hibridinių darinių savybės esminiai priklauso nuo pirmtako ir iškaitinimo atmosferos

Ginamieji teiginiai

1. Porėtojo n-Si sluoksnio morfologija esminiai priklauso nuo apšvietimo elektrocheminio ėsdinimo metu. Šią priklausomybę nulemia šviesa generuojamos skylės. Apšvietus ėsdinamą paviršių, skylės generuojamos tarpuose tarp porų ir skatina porų išsišakojimą. Apšviečiant apatinę padėklo pusę, skylės generuojamos tolygiai, todėl poros tolygiai gilėja ir jų diametras nekinta.
2. Hibridinių darinių por-Si pagrindu formavimąsi nulemia biomolekulių, turinčių sulfatines funkcines grupes, įsiterpimas į poras ir kovalentinių ryšių su silanolinėmis grupėmis, esančiomis porų paviršiuje, susidarymas.
3. Elektrocheminio ėsdinimo metu azoto rūgšties organiniame tirpiklyje ant GaP padėklo susiformuoja GaP nanostulpeliai (diametras ~100 nm, aukštis 3-10 μm). Nanostulpeliai susiformuoja iš por-GaP porų sienelių, kurioms suplonėjus iki nanometrinių dydžių, jų varža padidėja, o ėsdinimo greitis sumažėja. Visą por-GaP ėsdinimo procesą sudaro tokia morfologijos kitimo seka: poros GaP matricoje – korio pavidalo darinys – nanostulpeliai.
4. Fe/Fe-O nanodalelių, suformuotų zolis-gelis metodu porėtose SiO_2 matricose, savybės esminiai priklauso nuo atkaitinimo atmosferos. Nepriklausomai nuo oksidinės aplinkos sluoksnyje, kuriame yra laisvo deguonies, 550^{o}C temperatūroje atkaitinimas oksiduojančioje ir inertinėje atmosferoje skatina geležies oksidų nanodalelių susiformavimą, o redukuojančioje atmosferoje susidaro metalinės Fe nanoklasteriai.

Darbo apimtis. Disertacija sudaryta iš keturių skyrių. Pirmajame skyriuje išdėstytos darbe naudojamos matavimų metodikos. Kiti trys originalūs skyriai, kuriuose išdėstyti eksperimentinių darbų rezultatai ir atlikta jų analizė. Kiekvieno skyriaus pradžioje pateikiamas įvadas, kuriame pagrindžiamas medžiagos pasirinkimas, tyrimų

tikslas bei nusakomi galimi praktiniai taikymai. Pateikiami technologiniai ir eksperimentiniai tyrimai ir kiekvieno skyriaus pabaigoje pateikiamos trumpos to skyriaus išvados. Darbo pabaigoje pateikiamos bendros viso darbo išvados bei išspausdintų straipsnių ir dalyvautų konferencijų, kuriose buvo pristatomi darbo rezultatai, sąrašas. Taip pat pateikiamas visuose skyriuose naudotos literatūros sąrašas.

Pirmajame skyriuje aprašytos suformuotus darinius charakterizuoti naudotos metodikos.

Antrajame skyriuje pateikiama kontroliuojamos morfologijos porėtojo silicio sluoksnių gamybos technologija, suformuotų darinių morfologija, optinių savybių tyrimai bei porėtojo silicio pagrindu hibridinių nanodarinių formavimas.

Trečiajame skyriuje pateikiama porėtojo galio fosfido gamybos technologija, morfologijos ir optinių savybių tyrimai bei pateikiami dujų jutiklio porėtojo galio fosfido pagrindu sukūrimo galimybių tyrimai.

Ketvirtajame skyriuje aprašyti porėtųjų SiO_2 terpėje suformuotų Fe/Fe-O nanodalelių tyrimų rezultatai. Aptariama jų gamybos technologija, morfologijos, cheminės sudėties bei optinių savybių tyrimai.

Bendrosios išvados

1 n-tipo laidumo Si padėkluose porėtojo sluoksnio morfologija priklauso ne tik nuo darinių gamybos technologinių parametrų, bet ir nuo apšvietimo. Apšviečiant ėsdinamą paviršių kaitinimo lempa (λ_{max}=1,2 μm, 600 lx), susidaro poros, orientuotos statmenai į paviršių. Didinant apšvietimo intensyvumą (iki 1200 lx), poros šakojasi, persipina ir įgauna labai retą, netvarkingą struktūrą. Apšviečiant padėklą iš apatinės ėsdinamos plokštelės pusės, poros išsidėsto tvarkingai, jos vienodo ~2,5-3 μm dydžio. Tokį struktūros skirtumą sąlygoja šviesos generuojamų skylių sąlygos. Ėsdinimo metu apšviečiant ėsdinamą paviršių, skylės generuojamos tarpuose tarp susiformavusių porų, todėl porose atsiranda atsišakojimai. Tuo tarpu apšviečiant apatinę padėklo pusę, skylės generuojamos tolygiai apatiniame padėklo sluoksnyje ir elektrinio lauko veikiamos juda paviršiaus link. Pasiekusios poros dugną, jos oksiduoja Si atomus, ir poros dugne esantis silicis tirpsta. Tokiu atveju pora tolygiai gilėja, o jos diametras praktiškai nekinta.

2. Nusodintų iš vandeninio tirpalo porfirinų saviorganizacija ant įvairių padėklų skirtinga. Ant hidrofilinių paviršių susiformuoja ištisinis tolygus sluoksnis, sudarytas iš suaugusių į mezokompleksus J-agregatų ar FeTPPS dimerų. Ant dalinai hidrofobinių c-Si padėklų dėl paviršiaus neigiamo krūvio adsorbuojami teigiamą krūvį turintys agregatai formuoja orientuotą struktūrą. Geležies porfirinai ant dalinai hidrofobinio paviršiaus formuoja žiedus iš FeTPPS monomerų ir dimerinius nanodarinius žiedo viduje.

3. Por-GaP, formuojamo elektrocheminio ėsdinimo metodika, porų dydis ir morfologija esminiai priklauso nuo pasirinkto elektrolito tipo. Naudojant sieros rūgštį ir fluoro rūgštį, esant mažam srovės tankiui, buvo gauti būdingi tokiems elektrolitams dariniai. Struktūros, Naudojant sieros rūgštį, azoto rūgštį ir fluoro rūgštį, esant dideliam srovės tankiui buvo gautos pirmą kartą. Išmatuoti ir išanalizuoti por-GaP IR atspindžio spektrai liktinių spindulių srityje ir nustatyta spektrų smulkiosios struktūros koreliacija su bandinių morfologija. IR atspindžio spektrų forma priklauso nuo suformuotų darinių paviršiaus morfologijos ypatumų. Pirmą kartą elektrocheminio ėsdinimo metodu, naudojant azoto rūgšties elektrolitą, gauti 3-10 μm aukščio ir 100-400 nm pločio GaP

nanostulpeliai. Išbandytas dujų jutiklio prototipas por-GaP/ITO pagrindu, kurio varžinis jautrumas yra R_{ore} /$R_{garuose}$ =1.1.

4. Sukurta reguliuojamo porėtumo silicio oksido sluoksnių ant kristalinio Si (c-Si) padėklų formavimo zolis-gelis technologija, cheminio geležies ir jos junginių nanodalelių įterpimo į SiO_2 porėtuosius sluoksnius procedūra, geležies ir jos oksidų nanodalelių formavimo dielektrinėje matricoje, keičiant atkaitinimo sąlygas, metodika. Nustatyta, kad formuojant hibridinius darinius, viena vertus, galima kontroliuoti dielektrinės terpės porėtumą, keičiant prekursorių sąstatą ir technologinius rėžimus. Antra vertus, Fe/Fe-O nanodarinų ir klasterių formavimąsi galima valdyti tiek prekursoriu sudėtimi, tiek ir atkaitinimo procedūromis.

Trumpos žinios apie autorių

Marius Treideris gimė 1982 m. kovo 12 d. Vilniuje. 2004 metais Vilniaus universitete, Fizikos fakultete įgijo fizikos bakalauro laipsnį. Tais pačiais metais įstojo į Vilniaus universiteto Fizikos fakulteto magistratūrą ir ją baigęs (2006 m.) įgijo fizikos magistro kvalifikacinį laipsnį. 2006-2011 m. buvo Puslaidininkių fizikos instituto doktorantas. Nuo 2000 m. pradėjo dirbti Puslaidininkių fizikos institute laborantu, vėliau buvo inžinieriumi ir jaunesniuoju mokslo darbuotoju, pastarąsias pareigas užima iki šiol.